

Early evolution of the Earth–Moon system with a fast-spinning Earth



Jack Wisdom*, ZhenLiang Tian

Massachusetts Institute of Technology, Cambridge, MA 02139, USA

ARTICLE INFO

Article history:

Received 14 October 2014

Revised 21 February 2015

Accepted 22 February 2015

Available online 7 March 2015

Keywords:

Earth

Moon

Dynamics

ABSTRACT

The isotopic similarity of the Earth and Moon has motivated a recent investigation of the formation of the Moon with a fast-spinning Earth (Cuk, M., Stewart, S.T., [2012]. *Science*, doi:10.1126/science.1225542). Angular momentum was found to be drained from the system through a resonance between the Moon and Sun. They found a narrow range of parameters that gave results consistent with the current angular momentum of the Earth–Moon system. However, a tidal model was used that was described as approximating a constant Q tidal model, but it was not a constant Q model. Here we use a conventional constant Q tidal model to explore the process. We find that there is still a narrow range of parameters in which angular momentum is withdrawn from the system that corresponds roughly to the range found earlier, but the final angular momentum is too low to be consistent with the Earth–Moon system. Exploring a broader range of parameters we find a new phenomenon, not found in the earlier work, that extracts angular momentum from the Earth–Moon system over a broader range of parameters. The final angular momentum is more consistent with the actual angular momentum of the Earth–Moon system. We develop a simple model that exhibits the phenomenon.

© 2015 Elsevier Inc. All rights reserved.

1. Introduction

An isotopic crisis (Melosh, 2009) has inspired a recent scenario for the formation of the Moon (Cuk and Stewart, 2012). Prior research (Canup, 2004, 2008) into the giant impact scenario for the formation of the Moon has assumed that when the Moon was formed the Earth–Moon system was left with the present angular momentum. Indeed, this was thought to be a virtue of the model. However, in these simulations the Moon is predominantly formed from the impactor. Recent isotopic measurements have shown that the Moon and Earth have essentially identical isotopic composition for chromium (Lugmair and Shukolyukov, 1998), oxygen (Wiechert et al., 2001), tungsten (Touboul et al., 2007), and titanium (Zhang et al., 2012). Thus to explain the isotopic similarity of the Earth and Moon one has to appeal to an accidentally similar impactor, or to some sort of reequilibration of the isotopic signature after the impact but before the Moon formed (Pahlevan and Stevenson, 2007). But reequilibration of isotopes in the protolunar disk seems less likely because refractory isotopes have been found to be similar for the Earth and Moon. The similarity of the Earth and Moon suggests that the Moon forming impact was more severe than previously investigated and that the Moon formed from material derived directly from the Earth's mantle

(Cuk and Stewart, 2012; Canup, 2012). The problem is that such an impact would leave the Earth spinning much more rapidly than previously assumed and some mechanism of removing the excess angular momentum must be found.

One such mechanism was recently proposed by Cuk and Stewart (2012). In this scenario, the Moon is formed by a hard impact by a smaller and faster impactor than previously considered, excavating material that forms the Moon that is largely derived from Earth's mantle. The Moon is initially formed with low eccentricity just outside the Roche radius, and evolves outwards due to the action of tides on the Earth. As it evolves it is captured into a resonance between the Moon and the Sun where the period of precession of the lunar pericenter is one year. This resonance is called the evection resonance (see Touma and Wisdom, 1998). After the system is captured into the evection resonance the eccentricity of the lunar orbit rises dramatically. Due to the eccentricity damping effect of tides raised in the Moon (Goldreich, 1963), an equilibrium eccentricity is reached. In cases where the evection resonance is stable, angular momentum is drained from the system. The rotation rate of the Earth slows and the semimajor axis of the lunar orbit decreases until the angular orbital motion near pericenter matches the rotation rate of the Earth, at which point the evection resonance becomes unstable (Touma and Wisdom, 1998) and the system escapes from resonance. The angular momentum of the Earth–Moon system is left with a value close to the present angular momentum.

* Corresponding author.

E-mail addresses: wisdom@mit.edu (J. Wisdom), zlt@mit.edu (Z. Tian).

However, the tidal model used by Cuk and Stewart (2012) was described as approximating a “constant Q ” tidal model, but in fact it had little to do with a conventional constant Q tidal model. In this paper we show that when a conventional constant Q tidal model is used we can reproduce the basic phenomenon reported by Cuk and Stewart (2012), but too much angular momentum is lost. However, we have found an alternate scenario that can drain an appropriate amount of angular momentum from the system over a wide range of parameters.

2. Methods

The physical model and numerical methods that we use are similar to those used in Touma and Wisdom (1994, 1998), and also similar to those used by Cuk and Stewart (2012). One difference between our model and that of Cuk and Stewart is that we studied the rotation of the Moon (for reasons explained below); for Cuk and Stewart the Moon was a point mass.

Our numerical model integrates the orbital evolution of the Earth, Moon, and Sun. We integrate the full rotational dynamics of an axisymmetric Earth and a triaxial Moon, with spin–orbit coupling of Earth and Moon. We include tides in the Earth and Moon, using the constant- Q Darwin–Kaula model. We add intrinsic wobble damping following Peale (1977).

The symplectic mapping method of Wisdom and Holman (1991) forms the framework for our numerical model. In this method, the Hamiltonian is split into parts that are separately efficiently solvable; the complete evolution is obtained by interleaving the pieces. We think of the splitting in terms of the introduction of delta functions into the Hamiltonian. The n -body Hamiltonian is split into Kepler Hamiltonians plus the interaction Hamiltonian using hierarchical Jacobi coordinates (see Sussman and Wisdom, 2001). During the “drift” step we evolve both the Kepler motion and the free rigid body motion of the Earth and Moon. During the “kick” step the spin–orbit interactions are evaluated, and the tides are introduced by a tidal kick.

We actually developed two versions of our code. In one version the rotational configuration of each rigid body was specified by the rotation matrix that takes the body from its reference orientation to its actual orientation by an active rotation. In the other version we specified the rotational configuration by a quaternion (Sussman and Wisdom, 2001). The torques and accelerations are given by the expressions in Touma and Wisdom (1993). In the first code we evolved the free rigid body during the drift step using the Lie–Poisson algorithm specified in Touma and Wisdom (1993); in the second code we numerically integrated the quaternion equations of motion for a free rigid body (Sussman and Wisdom, 2001). We found that the two codes gave good agreement.

A key difference between our study and that of Cuk and Stewart is the tidal model. Cuk and Stewart used a tidal model that they described as approximating a constant Q tide, but it was not a constant Q tidal model; we actually used the conventional constant Q tidal model.

The Cuk and Stewart (2012) tidal model is as follows. The tidal torque on the Earth is

$$\mathbf{T} = -\frac{T_0 S(\omega, \dot{f})}{\omega r^6} \mathbf{M}, \quad (1)$$

where $S(\omega, \dot{f}) = (\omega - \dot{f}) / \sqrt{|\omega - \dot{f}|}$, and $T_0 = 1.95 \times 10^{-5}$ in units where Gm_e and R_e are unity. (The gravitational constant is G and the mass of the Earth is m_e . The radius of the Earth is R_e .) The quantity \mathbf{M} is the vector angular momentum of the Earth, ω is the rotation rate of the Earth, r is the Earth–Moon distance, and f is the true anomaly of the Moon’s orbit. The numerical value was chosen so that

the rate of evolution corresponded to $Q_e = 100$, where Q_e is the dissipation parameter for the Earth. Before we go on let’s criticize this expression. First, it is simply not the case that in any real tidal model the tidal torque is always aligned with the angular momentum vector. The tidal torque should involve the orbital elements (or the position and velocity) of the Moon, and the tidal torque need not be aligned with the angular momentum of the Earth. Second, the fact that the factor T_0 is given numerically, rather than being given in terms of parameters of the system, is indicative of the fact that this expression is not derived from more basic physical principles. Third, the origin of the factor S is not clear; its form seems to be completely arbitrary. Next, Cuk and Stewart state that “the acceleration of the Moon corresponds to a torque that is equal and opposite in sign.” Since a torque is derived from a force by a cross product, and information is lost in performing a cross product, it is not possible to uniquely determine the acceleration from the torque. Cuk and Stewart took the tidal acceleration to be perpendicular to the radius vector to resolve the ambiguity. Again, in conventional tidal models it is not necessarily the case that the tidal acceleration is perpendicular to the radius vector. Finally, the acceleration of the Moon due to tides raised in the Moon is given by the expression

$$\ddot{\mathbf{r}} = -\frac{A_0 v_r}{r^{13/2}} \hat{\mathbf{r}}, \quad (2)$$

where $A_0 = 2.7 \times 10^{-3}$ in the same units as before, and v_r is the radial component of the velocity. This has the virtue (and sole purpose) of damping the orbital eccentricity. It is not clear whether the eccentricity dependence of this tidal acceleration corresponds to any conventional tidal model. The factor A_0 is, again, not given in terms of physical parameters.

To illustrate these criticisms, consider the expressions for the popular constant Δt tide (see Touma and Wisdom, 1994, for a pedagogical introduction). In this tide (sometimes called the Mignard–Hut tide, Mignard (1979) and Hut (1981)), the response of the planet to the tide raising potential is a coherent tidal bulge that is delayed in time by a constant time interval Δt . The force on the Moon due to tides that it raises on the Earth is

$$\mathbf{F} = -\frac{3k_2 G M_m^2 R_e^5}{r^{10}} \{r^2 \mathbf{r} + \Delta t [2\mathbf{r}(\mathbf{r} \cdot \mathbf{v}) + r^2(\mathbf{r} \times \boldsymbol{\omega} + \mathbf{v})]\}, \quad (3)$$

and the torque on the Moon’s orbit (opposite to the torque on the Earth’s figure) is

$$\mathbf{T} = \mathbf{r} \times \mathbf{F} = -\frac{3k_2 G M_m^2 R_e^5 \Delta t}{r^{10}} [(\mathbf{r} \cdot \boldsymbol{\omega}) \mathbf{r} - r^2 \boldsymbol{\omega} + \mathbf{r} \times \mathbf{v}], \quad (4)$$

where \mathbf{r} is the vector from the Earth to the Moon, \mathbf{v} is the velocity of the Moon relative to the Earth, r is the magnitude of \mathbf{r} , and $\boldsymbol{\omega}$ is the angular velocity vector. Note that the coefficients are given in terms of physical parameters of the system; this reflects the fact that the expressions are derived from more basic physical principles. Note that there are three terms in the torque, only one of which is proportional to the angular momentum (spin) of the Earth. There are two other terms that involve the relative position and velocity of the Earth and Moon. The Cuk and Stewart torque is simply proportional to the angular momentum of the Earth. Note that the torque is derived from the force (acceleration) by performing a cross product of the radius vector with the force. The force is derived first. Cuk and Stewart reverse this: they evaluate the torque first and deduce the force from it with an extra assumption that the force is perpendicular to the radius. Of the four terms in the force, only one of them is perpendicular to the radius vector (the third). In the Cuk and Stewart tide the force is taken to be strictly perpendicular to the radius vector.

The constant Δt tide has the characteristics required of a real tidal model, but it does a poor job of fitting the Lunar Laser

Ranging results (Williams et al., 2005, 2014). Thus it is not a good tidal model for the Moon. The Mignard–Hut model is reported here because the expressions for it are simple and by comparison it illustrates deficiencies in the Cuk and Stewart tidal model.

We used a Darwin–Kaula constant Q model (Kaula, 1964). The Darwin–Kaula tidal model Fourier expands the tide raising potential and considers the response of the body on which tides are raised term by term. Each term in the tidal potential raises a tidal bulge and the corresponding exterior potential of that tidal bulge is proportional to the Love number k_l ; we keep only the second degree $l = 2$ terms. The response to each Fourier component is delayed in phase to take account of the dissipative nature of the tides. The Darwin–Kaula model is fully general in that it can represent the tidal response of a body with any rheology by incorporating the appropriate frequency dependence of the phase delays and the Love numbers.

But there is actually scant knowledge of the frequency dependence of the tidal response of planets and satellites. Indeed, only for the Moon is there any hint of the frequency dependence of the tidal response, and there the response is measured for only two frequencies. The result is a weak dependence on frequency (Williams et al., 2005, 2014). According to these Lunar Laser Ranging (LLR) results, the lunar Q at one month is 30, and the lunar Q at one year is 34. The expression for the Q as a power law is $30(\text{Period}/27.212\text{d})^{0.04}$. Thus the lunar Q is very nearly independent of frequency. Williams et al. (2014) state “The uncertainties at 1 month and 1 year are too large to assess whether dissipation increases or decreases with period.” The frequency dependence of the tidal response of the early Moon and Earth are unknown. In view of this uncertainty, with the LLR results, we adopt the “constant Q ” model, as proposed by Kaula (1964) and Goldreich (1966). Also, we adopt the constant Q model because this is the model the Cuk and Stewart model was intended to approximate. Note that the constant Δt tide has $Q \propto \text{Period}$ and so is not a good match to the LLR results (Williams et al., 2014).

The general expression for the tidal potential is (Kaula, 1964):

$$T(r, \phi, \lambda) = \sum_{lmpq} T_{lmpq}(r, \phi, \lambda), \quad (5)$$

where r is the radial distance from the center of the planet on which tides are raised, ϕ and λ are respectively, the latitude and longitude of the point of evaluation of the tidal potential. We restrict l to 2, m and p run from 0 to l , and q runs from $-N$ to N . Note that higher $|q|$ terms are proportional to a higher power of eccentricity e . We chose $N = 10$, to be intentionally excessive. The components of the tidal potential are:

$$\begin{aligned} T_{lmpq}(r, \phi, \lambda) &= \left(\frac{R}{r}\right)^{l+1} k_l [U_{lmpq}(R)]_{\text{lag}} \\ &= k_l \frac{R^{2l+1}}{r^{l+1}} B_{lm}^* C_{lmpq}^* P_{lm}(\sin \phi) \\ &\quad \times \begin{cases} \cos \\ \sin \end{cases}_{l-m \text{ even/odd}} (v_{lmpq}^* - \epsilon_{lmpq} - m(\lambda + \theta^*)), \end{aligned} \quad (6) \quad (7)$$

where R is the radius of the planet on which tides are being raised, k_l is the potential Love number, U_{lmpq} is the $lmpq$ component of the tide raising potential, “lag” indicates that the phase of each term is lagged to take account of dissipation. In the subsequent expression, we have

$$B_{lm}^* = Gm^* \frac{(l-m)!}{(l+m)!} (2 - \delta_{0m}), \quad (8)$$

$$C_{lmpq}^* = \frac{1}{(a^*)^{l+1}} F_{lmp}(i^*) G_{lpq}(e^*), \quad (9)$$

$$v_{lmpq}^* = (l-2p)\omega^* + (l-2p+q)M^* + m\Omega^*, \quad (10)$$

where, in general, the asterisk marks quantities belonging to the tide raising body, and ω is argument of pericenter, M is the mean

anomaly, Ω is the longitude of the ascending node, and θ is the angle from the inertial reference longitude to the origin of longitudes on the planet on which tides are raised. The Kaula inclination polynomials $F_{lmp}(i^*)$ for $l = 2$ are tabulated in Kaula (1964); the eccentricity functions $G_{lpq}(e^*)$ may be written in terms of Hansen functions:

$$G_{lpq}(e^*) = X_{l-2p+q}^{-(l+1), (l-2p)}(e^*). \quad (11)$$

The Hansen functions, when written as a power series in the eccentricity, have the Newcomb coefficients as coefficients. The lowest order Hansen functions are listed in Kaula (1964). More generally, the Newcomb coefficients (and hence the Hansen functions) may be evaluated with a simple recurrence (Plummer, 1960). Because these are needed many times (each time the tidal potential is evaluated) we “memoized” the table of Newcomb coefficients, i.e. we computed only the coefficients that were needed, as needed, and the computed values were saved in a table for later use. We evaluated the Hansen functions up to order 10 in the eccentricity. The accelerations and torques are derived from this tidal potential.

The “constant Q ” tide is a specialization of this general expression in which the phase lags ϵ_{lmpq} are taken to be all equal in magnitude ϵ with the sign of $(\dot{v}_{lmpq} - m\dot{\theta})$. The ϵ is related to Q by $\tan \epsilon = 1/Q$. Note how little the Cuk and Stewart “constant Q ” tidal model has in common with the actual constant Q tide.

There is a tidal torque on the Moon that tends to remove the Moon from synchronous rotation. But because the figure of the Moon is out-of-round the synchronous lock remains. What results, in the simplest situation, is that there is an offset in the direction of the axis of minimum moment from the line pointing to the Earth. This offset results in additional forces on the Earth–Moon orbit. If the Moon’s rotation remains simple, then these additional torques can be calculated and taken into account in the equations of tidal evolution (Yoder and Peale, 1981). But, more generally, they can be taken into account by actually integrating the rotation of the Moon and the resulting spin–orbit interactions. We chose the latter course because it is more general.

3. Evection resonance results

Figs. 1 and 2 show aspects of the evolution of the Earth–Moon system in a simulation with $Q_e = 100$ and $A = 1.7376$. The A parameter is a measure of the relative dissipation in the Earth and the Moon:

$$A = \frac{k_{2m}}{Q_m} \frac{Q_e}{k_{2e}} \frac{m_e^2}{m_m^2} \frac{R_m^5}{R_e^5}, \quad (12)$$

where k_{2i} are the second order potential Love numbers of the Moon ($i = m$) and the Earth ($i = e$), Q_i are the dissipation factors, m_i are the masses, and R_i are the radii. A small A implies relatively small dissipation in the Moon; a large A implies relatively large dissipation in the Moon. In this simulation the obliquity of the Earth and Moon, and inclination of the Moon’s orbit are all zero. Because of the assumption of Cuk and Stewart (2012) that the tidal torque is proportional to the angular momentum the domain of applicability is restricted to zero inclination and obliquity. So we first compare our results for zero obliquities and lunar inclination to the results of Cuk and Stewart (2012). In this simulation the initial Earth–Moon separation is $5R_e$, with initial rotation period of 2.53 h. This corresponds to an evolution from an initial Earth–Moon separation of $3.5R_e$ with an initial rotation period of 2.5 h, we just saved time by starting the evolution a little further out.

The orbital eccentricity (see Fig. 1) shows a sudden increase upon entering the evection resonance (see Touma and Wisdom, 1998, for analytic approximations to the evolution in the evection

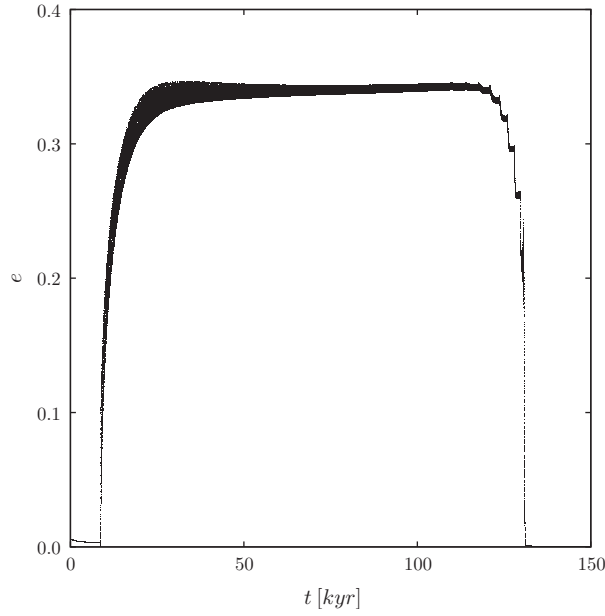


Fig. 1. The eccentricity e of the lunar orbit is plotted versus time t . For this run $Q_e = 100$ and $A = 1.7376$. The obliquity is zero.

resonance). The eccentricity reaches an equilibrium in which the tendency to increase in the evection resonance is balanced by a tendency to decrease due to dissipation in the Moon. This is followed by an interval of approximately 130,000 years of nearly constant large eccentricity. Over this interval the semimajor axis and the rotation rate of the Earth decrease. Once the system escapes the evection resonance the eccentricity quickly gets small. The plot of the evection resonance angle (see Fig. 2) shows that once the system is captured the resonance angle, $\sigma = \varpi - \lambda_\odot$, librates about, in this case, $\pi/2$, and the amplitude of the libration gradually decreases. Here, ϖ is the longitude of pericenter of the lunar orbit, and λ_\odot is the longitude of the Earth in its orbit about the Sun. Whether the system is captured about $\pi/2$ or $3\pi/2$ is probabilistic.

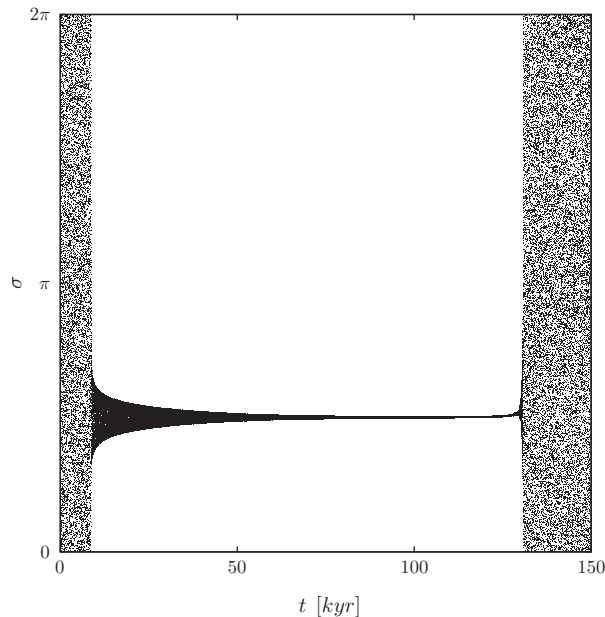


Fig. 2. The evection resonant argument σ is plotted versus time t . For this run $Q_e = 100$ and $A = 1.7376$. The obliquity is zero.

These results are all roughly consistent with those of Cuk and Stewart (2012), though the details differ.

An important difference with respect to Cuk and Stewart (2012) is the amount of angular momentum that is extracted from the system as a result of this temporary capture into the evection resonance. Fig. 3 shows the final angular momentum versus A from Cuk and Stewart (2012) and for our model, which uses a true constant Q tide. We see that with the full model too much angular momentum is withdrawn from the system to be consistent with the Earth–Moon system.

4. Evection resonance results with inclination and obliquity

Unlike the Cuk and Stewart tidal model, our model is fully general in that it can handle arbitrary obliquities and lunar inclination. It is known that to be consistent with today's inclination of the lunar orbit to the ecliptic the Moon had a 10° inclination to the equator of the Earth at about $10R_e$, and the obliquity of the Earth at this point had to be about 10° (see Touma and Wisdom, 1994, 1998). We have made some initial explorations of the process of passage through the evection resonance with nonzero initial obliquity and inclination.

In this exploration we started the Moon with an inclination to the Earth's equatorial plane of 9.9° ; the initial obliquity of the Earth is 10° . The initial rotation period of the Earth of 2.5 h. The initial eccentricity of the lunar orbit is 0.001 and the semimajor axis is $a = 3.5R_e$.

The plots of the orbital elements are similar to the zero obliquity plots, though naturally a little more complicated, and will not be shown in detail. One result is that we found that wobble of the Moon is significantly excited. There are two sources of wobble damping in the Moon. It turns out that tides on the Moon raised

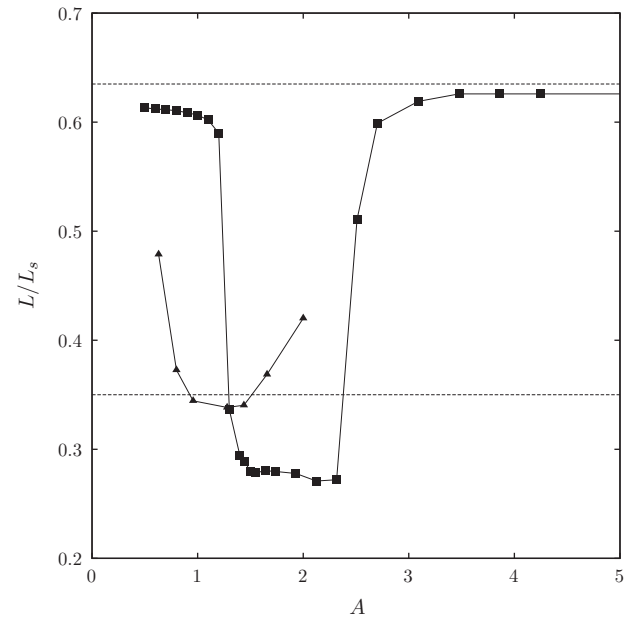


Fig. 3. This plot shows the scaled angular momentum of the Earth–Moon system L/L_s after the system escapes the evection resonance versus the A parameter. The angular momentum scale is $L_s = C\sqrt{Gm_e/(R_e^3)}$, where C is the largest moment of inertial of Earth, m_e is the mass of the Earth, and R_e is the radius of the Earth. The filled triangles are the results of Cuk and Stewart (2012), who used their own tidal model. The filled squares are our results using the conventional constant Q model. For our results to be comparable to those of Cuk and Stewart we have taken the obliquities and inclination to be zero. The horizontal line near $L/L_s = 0.35$ indicates the current angular momentum of the Earth–Moon system; the line $L/L_s = 0.635$ is the initial scaled angular momentum in our runs.

by the Earth damp wobble in the Moon (Peale, 1976). Another source of wobble damping is internal dissipation in the Moon (Peale, 1977). We include both of these mechanisms of wobble damping in our simulations.

We adopt a simple model for intrinsic wobble damping. In isolation, intrinsic wobble damping conserves angular momentum but damps body components of the angular velocity. Let $A \leq B \leq C$ be the principal moments of inertia, and ω^a, ω^b , and ω^c be the corresponding components of the angular velocity. The body components of the angular momentum are $L_a = A\omega^a$, $L_b = B\omega^b$, and $L_c = C\omega^c$. We then calculate $\omega'_a = \omega_a \exp(-\Delta t/\tau)$, and $\omega'_b = \omega_b \exp(-\Delta t/\tau)$, for time interval Δt and time constant τ . Then define $L'_a = A\omega'_a$, $L'_b = B\omega'_b$, and $L'_c = C\omega'_c = C\omega_c$. Let $L = \sqrt{L_a^2 + L_b^2 + L_c^2}$ and $L' = \sqrt{(L'_a)^2 + (L'_b)^2 + (L'_c)^2}$, then $L''_a = L'_a(L/L')$, $L''_b = L'_b(L/L')$, $L''_c = L'_c(L/L')$. From this we can compute the new components of the angular velocity on the principal axes: $(\omega'')^a = L''_a/A$, $(\omega'')^b = L''_b/B$, $(\omega'')^c = L''_c/C$. But the principal axes need to be rotated to bring the new angular momentum components into alignment with the direction of the angular momentum in space, which does not change. Define $\mathbf{q} = (\mathbf{L}'' \times \mathbf{L})/(\mathbf{L}'' \cdot \mathbf{L})$, where the boldface indicates vectors in the body frame. Let $\sin \alpha$ be the length of \mathbf{q} ; α is the angle between the directions of \mathbf{L} and \mathbf{L}'' . Then let $\hat{\mathbf{q}} = \mathbf{q}/(\sin \alpha)$ be the unit vector about which we rotate the body in inertial space by the angle α to bring the new body components of the angular momentum into alignment with the original angular momentum. The net result is a body with the original angular momentum, but with smaller components of the angular velocity on the \hat{a} and \hat{b} axes. The timescale for wobble damping is (Peale, 1977):

$$\tau = \frac{3G C Q}{k_2 R^5 \omega^3}, \quad (13)$$

where G is the gravitational constant, k_2 is the potential Love number, Q is the tidal dissipation parameter, R is the radius, and ω is the rotation rate.

We quantify wobble by the ratio of the magnitude of the component of the angular velocity on the \hat{a} and \hat{b} plane (where \hat{a} and \hat{b} are the axes of minimum and intermediate moments of inertia) divided by the total angular velocity. Let

$$\omega_{ab} = (\omega_a^2 + \omega_b^2)^{1/2}, \quad (14)$$

and

$$\omega = (\omega_a^2 + \omega_b^2 + \omega_c^2)^{1/2}, \quad (15)$$

then a dimensionless measure of the amount of wobble is ω_{ab}/ω . Fig. 4 shows a plot of this measure of the wobble versus time for a run with obliquities and lunar inclination.

We expect that the Moon will have a 200–400 km deep magma ocean overlain by a 5–10 km crust during the interval in which the evection resonance is encountered (Elkins-Tanton, 2008). The interior below the magma ocean is solid. It is not clear that the rigid body dynamics we have assumed is an adequate description of the dynamics of a body with such complicated structure. We might expect that it would be harder to maintain wobble in a body with a magma ocean. So we have carried out a series of runs with the rate of wobble damping enhanced by a factor of 10. This is enough to eliminate the wobble instabilities seen in the first set of runs. Note that Peale (1977) acknowledges that other estimates of the wobble damping timescale are as much as an order of magnitude smaller than his estimate.

Fig. 5 shows a summary of the final angular momentum in the runs in this interval of the A parameter, for $Q_e = 100$. The results with zero obliquity and inclination are shown with the results

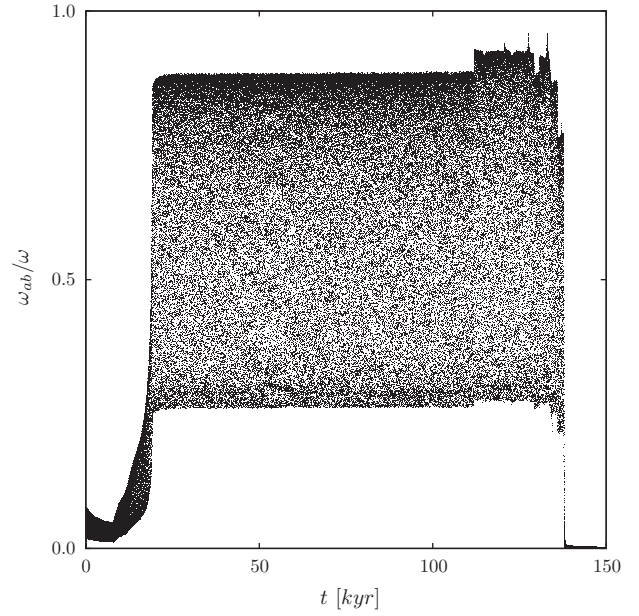


Fig. 4. The wobble ω_{ab} of the Moon is plotted versus time t . For this run $Q_e = 100$ and $A = 2.319$. The initial obliquity of the Earth is 10° and the inclination of the lunar orbit to the equator of the Earth is 9.9° .

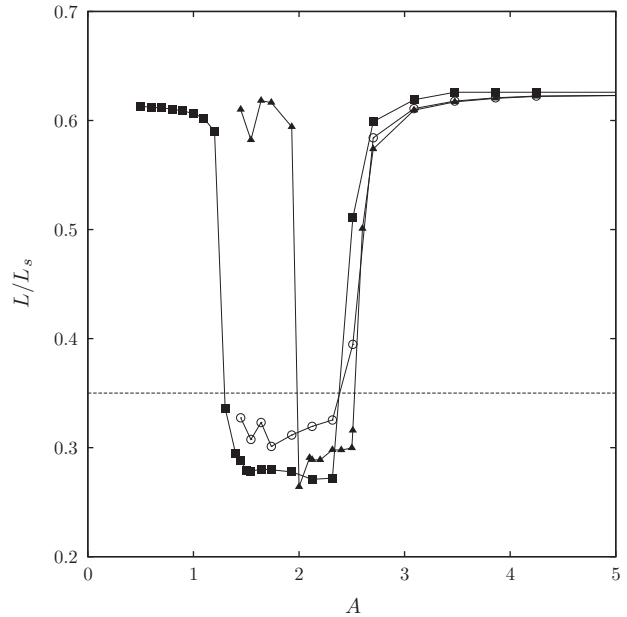


Fig. 5. This plot shows the scaled angular momentum of the Earth–Moon system L/L_s after the system escapes the evection resonance versus the A parameter. The filled squares are the zero obliquity results. The filled triangles are our results with initial Earth obliquity of 10° and initial lunar inclination to the equator plane of 9.9° . The open circles are our results with obliquity and inclination, but with enhanced wobble damping. The horizontal line near $L/L_s = 0.35$ indicates the current angular momentum of the Earth–Moon system.

for the oblique, inclined case, with and without enhanced wobble damping. It is still the case that too much angular momentum is extracted when the system is captured by the evection resonance to be consistent with the Earth–Moon system. Of course, this is just one tidal model; perhaps other tidal models would give a final angular momentum that is more consistent with the actual angular momentum of the Earth–Moon system.

5. A limit cycle

We have explored a wider range of parameters than were explored by Cuk and Stewart (2012), and we found a new dynamical phenomenon that may be more promising for the explanation of the Earth–Moon angular momentum than the scenario proposed by Cuk and Stewart. We found that for larger A and larger Q_e the system bypasses the evection resonance, and gets caught in what might best be called a limit cycle associated with the evection resonance. The system is not captured in the evection resonance, but instead the evection resonant argument circulates. The rate of evolution of the evection resonant argument is modulated by the phase of the resonant argument. In the phase plane ($e \cos \sigma, e \sin \sigma$), the system circulates around the libration islands associated with the evection resonance. It appears to be an attracting cycle, thus the proposed name of “limit cycle.”

The eccentricity e versus time t for the limit cycle is shown in Fig. 6. For this run we set the obliquities of the Earth and Moon, and the lunar inclination, to zero. We see that the eccentricity is caught in a cycle, and that both the maximum and minimum eccentricity of this cycle are much smaller than the equilibrium eccentricity when the system is caught in the evection resonance. The stroboscopic plot of the evection resonance angle σ versus time t (Fig. 7) shows that the resonance angle circulates (the system is not caught in the evection resonance), and that the rate of evolution is modulated by the phase of the evection resonance angle.

Fig. 8 shows the angular momentum versus A after the limit cycle is passed. In these runs, the initial obliquities and lunar inclination were set to zero, and $Q_e = 400$. For $Q_e = 100$ we did not find the limit cycle behavior over this same range of A . We see that over a broad range of A , roughly $8 < A < 15$, significant angular momentum is extracted from the system. Recall that additional angular momentum is extracted from the system by solar tides as the system evolves from $10R_e$, where these simulations were terminated, to the present $60R_e$, though the extent of this additional angular momentum extraction surely depends on the tidal model. So it is appropriate that the limit cycle results lie above the Earth–Moon line.

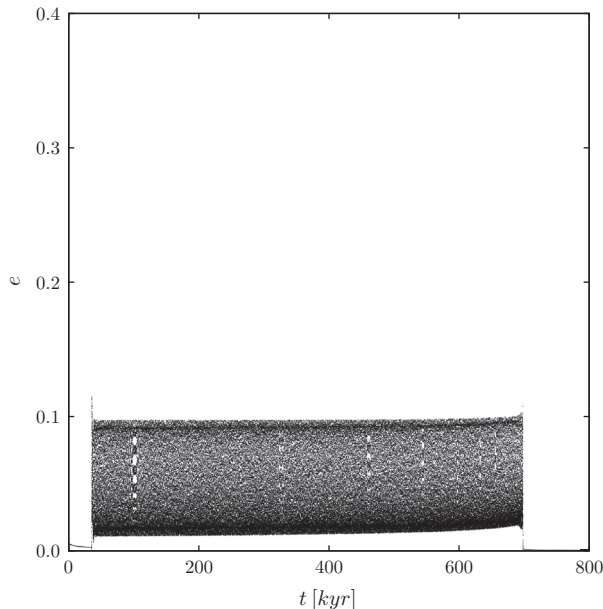


Fig. 6. The limit cycle is exhibited in this plot of eccentricity e versus time t . In this run the obliquities and lunar inclination are zero. This run uses the full model with $Q_e = 400$ and $A = 13.0$.

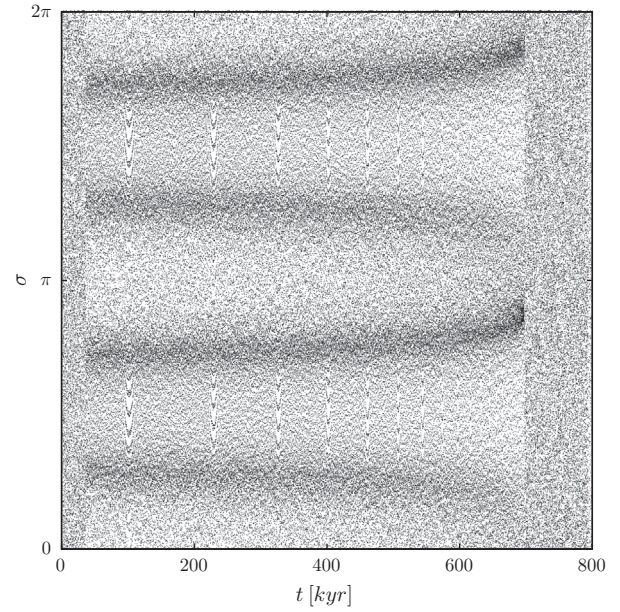


Fig. 7. The limit cycle is exhibited in this plot of resonant argument σ versus time t . The resonant argument circulates and is sampled at regular intervals. Concentrations of points occur at angles at which the evolution of the resonant argument is slower. In this run the obliquities and lunar inclination are zero. This run uses the full model with $Q_e = 400$ and $A = 13.0$.

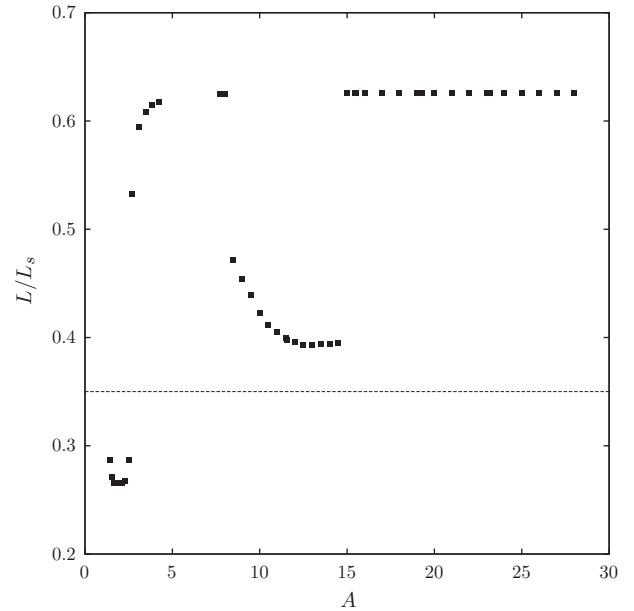


Fig. 8. This plot shows the scaled angular momentum after passage through the limit cycle versus the dissipation parameter A . In these runs with the full model, the obliquities and lunar inclination are set to zero, and $Q_e = 400$. We see a broad range of A in which significant angular momentum is extracted from the system. The horizontal line indicates the present angular momentum of the Earth–Moon system.

We have also found that the limit cycle behavior exists for $Q_e = 400$ when the obliquities and lunar inclination are nonzero.

6. A simplified model of the limit cycle

The behavior in the limit cycle can be captured to some extent by a simplified model. In this simplified model, we take the obliquities of the Earth and Moon, and the inclination of the lunar orbit

to the equator plane of the Earth all to be zero. The Hamiltonian governing the behavior near the evection resonance (see [Touma and Wisdom, 1998](#)) is then

$$H = n_2 \Sigma - \frac{1}{2} n_1 J_2 \left(\frac{R_e}{a_1} \right)^2 L' \frac{1}{(1-e^2)^{3/2}} - \frac{n_2^2 L' e^2}{n_1} \frac{15}{8} \cos 2\sigma, \quad (16)$$

where $\Sigma = L'(1 - (1 - e^2)^{1/2})$ is the momentum conjugate to the evection angle $\sigma = n_2 t - \varpi$, where ϖ is the longitude of the pericenter, and where $L' = (m_1 \mu a_1)^{1/2}$, with $\mu = Gm_1 m_2 / n_2$ is the mean motion of the Earth about the Sun, m_1 is the mass of the Moon, m_2 is the mass of the Earth, n_1 is the mean motion of the Moon about the Earth, J_2 is the Earth oblateness factor, R_e is the equatorial radius of the Earth, and e is the orbital eccentricity of the Moon. Note that

$$e^2 = \frac{\Sigma}{L'} \left(2 - \frac{\Sigma}{L'} \right). \quad (17)$$

We assume that $J_2 = J_{20}(\omega/\omega_0)^2$ where ω is angular rate of rotation of the Earth. We assume $J_{20} = 0.001083$ for ω_0 corresponding to a 24 h rotation. We express the Hamiltonian in terms of the non-singular momentum $\xi = \sqrt{2\Sigma} \cos \sigma$ and conjugate coordinate $\eta = \sqrt{2\Sigma} \sin \sigma$. The equations of motion are just Hamilton's equations.

To Hamilton's equations we add terms that reflect the tidal evolution. These are derived from the constant Q Darwin–Kaula model ([Kaula, 1964](#)).

Based on the Kaula series, we might naively write

$$\frac{da}{dt} = \frac{2}{3} K a \left(1 - \left(19A - \frac{51}{4} \right) e^2 + \left(\frac{1065}{16} - \frac{551}{8} A \right) e^4 + \dots \right), \quad (18)$$

$$\frac{de}{dt} = -\frac{1}{3} K \left(\left(7A - \frac{19}{4} \right) e + \left(\frac{299}{8} A - \frac{503}{16} \right) e^3 + \dots \right), \quad (19)$$

where

$$K = \frac{9}{2} \frac{k_{2e}}{Q_e} \frac{m_m}{m_e} \sqrt{\frac{Gm_e}{R_e^3}} \left(\frac{R_e}{a} \right)^{13/2}, \quad (20)$$

and where k_{2i} are the second order potential Love numbers of the Moon ($i = m$) and the Earth ($i = e$), Q_i are the dissipation factors, m_i are the masses, and R_i are the radii.

But tides on the Moon have a net torque on the Moon that tends to remove the Moon from synchronous rotation. If the Moon's minimum moment of inertia is not aligned with the Earth, then the Moon is subject to a gravity gradient torque because of its nonzero gravitational moment C_{22} . In the equilibrium orientation of the Moon these two torques balance. This orientation offset results in additional terms in the equations governing the evolution of the lunar orbit. These additional terms can either be taken into account by integrating the rotation of the Moon, as we did in the full model, or by modifying the expressions for the tidal evolution of the semimajor axis and eccentricity. Here we follow the latter course. Taking this effect into account, the total rate of change of the semimajor axis and eccentricity of the Moon are

$$\frac{da}{dt} = \frac{2}{3} K a (1 + c_2 e^2 + c_4 e^4 + c_6 e^6 + \dots), \quad (21)$$

$$\frac{de}{dt} = -\frac{1}{3} K (d_1 e + d_3 e^3 + d_5 e^5 + \dots). \quad (22)$$

For $(5/2)n < \omega$, the coefficients are:

$$c_2 = \frac{51}{4} - 7A, \quad (23)$$

$$c_4 = \frac{1065}{16} - \frac{403}{8} A, \quad (24)$$

$$c_6 = \frac{29229}{128} - \frac{1207}{6} A, \quad (25)$$

and

$$d_1 = 7A - \frac{19}{4}, \quad (26)$$

$$d_3 = \frac{347}{8} A - \frac{503}{16}, \quad (27)$$

$$d_5 = \frac{3619}{24} A + \frac{14117}{128}. \quad (28)$$

For $2n < \omega < (5/2)n$, the coefficients are:

$$c_2 = \frac{51}{4} - 7A, \quad (29)$$

$$c_4 = \frac{1065}{16} - \frac{403}{8} A, \quad (30)$$

$$c_6 = -\frac{3044003}{2304} - \frac{1207}{6} A, \quad (31)$$

and

$$d_1 = 7A - \frac{19}{4}, \quad (32)$$

$$d_3 = \frac{347}{8} A - \frac{503}{16}, \quad (33)$$

$$d_5 = \frac{3619}{24} A + \frac{629323}{768}. \quad (34)$$

For $(3/2)n < \omega < 2n$, the coefficients are:

$$c_2 = \frac{51}{4} - 7A, \quad (35)$$

$$c_4 = -\frac{3559}{16} - \frac{403}{8} A, \quad (36)$$

$$c_6 = -\frac{41123}{2304} - \frac{1207}{6} A, \quad (37)$$

and

$$d_1 = 7A - \frac{19}{4}, \quad (38)$$

$$d_3 = \frac{347}{8} A + \frac{1809}{16}, \quad (39)$$

$$d_5 = \frac{3619}{24} A - \frac{37621}{768}. \quad (40)$$

These results generalize the result used in [Yoder and Peale \(1981\)](#).

Though we have reported these expressions for various conditions on the rotation rate relative to the lunar mean motion, it turns out that these were not needed. For the evolution in the limit cycle the condition $(5/2)n < \omega$ is always maintained; there are no changes in the values of the tidal constants during the evolution.

To these tidal orbital equations we must add an equation for the tidal slowing of the rotation of the Earth. We find

$$\frac{d\omega}{dt} = -\frac{L}{\lambda M_e R_e^2} \left(\frac{1}{2a} \frac{da}{dt} - \frac{e}{1-e^2} \frac{de}{dt} \right), \quad (41)$$

where $\lambda = C/(M_e R_e^2) = 0.3308$, with polar moment of inertia C , and $L = L'(1 - e^2)^{1/2}$.

The simple model captures the evolution into the limit cycle. This demonstrates that the limit cycle is not an artifact of the rather complicated full model. But the agreement with full model is not as good as one would have hoped. First, the range of eccentricity variation is shifted to larger values in the simplified model. The eccentricity reaches values near 0.16 for the simplified model, but only values near 0.1 for the full model. Also, the range of the A parameter in which the limit cycle phenomenon occurs is different for the simplified model and the full model. [Fig. 9](#) shows the summary plot of scaled angular momentum versus the A parameter for the simplified model. We do not yet understand why there is this disagreement. Presumably, the full model captures some physical effect that we have not identified for inclusion in the simple model.

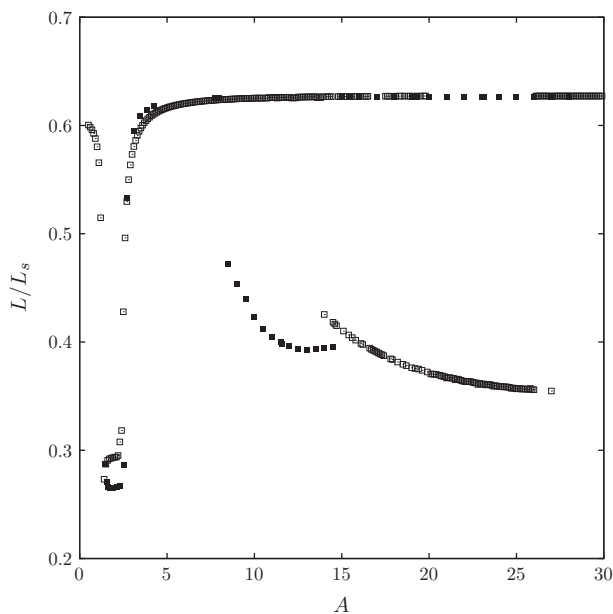


Fig. 9. Results of the simplified model with $Q_e = 400$. The open squares mark the results using the simplified model; the filled squares mark the results of the full model. The limit cycle is found with the simplified model, though the results do not match the full model exactly. Note that capture by the limit cycle is probabilistic for some values of A .

But the fact that the simple model exhibits the limit cycle is important, nevertheless.

7. Discussion

We are concerned that the high eccentricities obtained during the temporary capture in the evection resonance (e of order 0.35) would lead to large tidal heating, which in turn would change the parameters of the Moon and the consequent orbital evolution. Recall that the formula for tidal heating (Peale and Cassen, 1979) is proportional to the square of the orbital eccentricity and inversely proportional to sixth power of the semimajor axis. During the temporary capture in the evection resonance the eccentricity is high and the semimajor axis is small, so we can expect large tidal heating. Of course, the Moon is expected to have a thin (5–10 km) lid underlain by a magma ocean (200–400 km) during the interval in which the system is captured by the evection resonance. This configuration may be expected to actually increase the tidal heating, as heating in a thin lid can actually be larger than in a corresponding solid body (Peale et al., 1979). To properly address the consequences of this tidal heating on the orbital evolution requires examining a coupled thermal–orbital model, which we plan to do in a subsequent work.

Note however that the limit cycle behavior that we have discovered has an advantage in this regard. The typical eccentricity is less than of order 0.1. So according to the tidal heating formula, the rate of tidal heating, all other factors remaining the same, would be less by a factor of about 10. So the concern about tidal heating affecting the orbital evolution is mitigated, to some extent. The problem should still be addressed in a coupled thermal–orbital model.

8. Conclusion

The tidal model of Cuk and Stewart (2012) was described as approximating a constant Q tide, but, in fact, had little to do with a constant Q tide. We have explored the early evolution of the Earth–Moon system through the evection resonance with a true

constant Q tide. We found that we can reproduce the basic phenomenon discovered by Cuk and Stewart (2012), which is that significant angular momentum can be extracted from the system. However, we find that the evection resonance actually extracts too much angular momentum to be consistent with the current Earth–Moon system. Exploring a broader range of parameters than explored by Cuk and Stewart (2012), we found a new phenomenon, which we describe as a limit cycle of the evection resonance. The resonant argument of the evection resonance is not oscillating, but rather is circulating in a manner that is modulated by the phase of the evection resonant argument. Angular momentum is also extracted from the Earth–Moon system if the system is captured by the limit cycle. We find that after the system escapes the limit cycle the angular momentum is a little larger than the current angular momentum of the Earth–Moon system, but this is good as during the subsequent evolution to the present configuration solar tides continue to extract a small amount of angular momentum. The range of parameters that give an appropriate reduction of angular momentum is broader than the range of parameters for which the evection resonance reduces the angular momentum. Of course, other tidal models should be explored. We feel that the limit cycle holds promise for explaining the angular momentum of the Earth–Moon system, in the context of the new scenarios for harder Moon-forming impacts.

Acknowledgment

We thank M. Cuk, S. Stewart, J. Meyer, and W. Ward for interesting and helpful discussions.

References

- Canup, R.M., 2004. Simulations of a late lunar-forming impact. *Icarus* 168, 433–456.
- Canup, R.M., 2008. Lunar-forming collisions with pre-impact rotation. *Icarus* 196, 518–538.
- Canup, R.M., 2012. Forming a Moon with an Earth-like composition via a giant impact. *Science*. <http://dx.doi.org/10.1126/science.1226073>.
- Cuk, M., Stewart, S.T., 2012. Making a Moon from a fast-spinning Earth: A giant impact followed by resonance despinning. *Science*. <http://dx.doi.org/10.1126/science.1225542>.
- Elkins-Tanton, L.T., 2008. Linked magma ocean solidification and atmospheric growth for Earth and Mars. *Earth Planet. Sci. Lett.* 271, 181–191.
- Goldreich, P., 1963. On the eccentricity of satellite orbits in the Solar System. *Mon. Not. R. Astron. Soc.* 126, 257–268.
- Goldreich, P., 1966. History of the lunar orbit. *Rev. Geophys. Space Phys.* 4, 411–439.
- Hut, P., 1981. Tidal evolution in close binary systems. *Astron. Astrophys.* 99, 126–140.
- Kaula, W.M., 1964. Tidal dissipation by solid friction and the resulting orbital evolution. *Rev. Geophys. Space Phys.* 2, 661–685.
- Lugmair, G.W., Shukolyukov, A., 1998. Early Solar System timescales according to ^{53}Mn – ^{53}Cr systematics. *Geochim. Cosmochim.* 62, 2863–2886.
- Melosh, H.J., 2009. An isotopic crisis for the giant impact origin of the Moon? In: *Annual Meeting of the Meteoritical Society LXXII*, p. 5104.
- Mignard, F., 1979. The evolution of the lunar orbit revisited. I. *Moon Planets* 20, 301–315.
- Pahlevan, K., Stevenson, D.J., 2007. Equilibration in the aftermath of the lunar-forming giant impact. *Earth Planet. Sci. Lett.* 262, 438–449.
- Peale, S.J., 1976. Excitation and relaxation of the wobble, precession, and libration of the Moon. *J. Geophys. Res.* 81, 1813–1827.
- Peale, S.J., 1977. Rotation histories of the natural satellites. U. Arizona.
- Peale, S.J., Cassen, P., 1979. Contribution of tidal dissipation to lunar thermal history. *Icarus* 36, 245–269.
- Peale, S.J., Cassen, P., Reynolds, R., 1979. Melting of 10 by tidal dissipation. *Science* 203, 892–894.
- Plummer, H.C., 1960. *An Introductory Treatise on Dynamical Astronomy*. Dover.
- Sussman, G.J., Wisdom, J., 2001. *Structure and Interpretation of Classical Mechanics*. MIT Press.
- Touboul, M. et al., 2007. Late formation and prolonged differentiation of the Moon inferred from W isotopes in lunar metals. *Nature* 450, 1206–1209.
- Touma, J., Wisdom, J., 1993. Lie–Poisson integrators for rigid body dynamics in the Solar System. *Astron. J.* 107, 1189–1202.
- Touma, J., Wisdom, J., 1994. Evolution of the Earth–Moon system. *Astron. J.* 108, 1943–1961.
- Touma, J., Wisdom, J., 1998. Resonances in the early evolution of the Earth–Moon system. *Astron. J.* 115, 1653–1663.

- Wiechert, U. et al., 2001. Oxygen isotopes and the Moon forming giant impact. *Science* 294, 345–348.
- Williams, J.G., Boggs, D.H., Ratcliff, J.T., 2005. Lunar fluid core and solid-body tides. In: LPSC XXXVI, p. 1503.
- Williams, J.G. et al., 2014. Lunar interior properties from the GRAIL mission. *JGR Planets* 119, 1546–1578.
- Wisdom, J., Holman, M., 1991. Symplectic maps for the N-body problem. *Astron. J.* 102, 1528–1538.
- Yoder, C., Peale, S.J., 1981. The tides of Io. *Icarus* 47, 1–35.
- Zhang, J. et al., 2012. The proto-Earth as a significant source of lunar material. *Nat. Geosci.* 5, 251–255.